

Sea Surface Temperature (SST) and Rainfall Trends in the Singapore Strait from 2002 to 2019

Mubarak Mubarak^{1*}, Rifardi Rifardi¹, Ahmad Nurhuda¹, Romi Fadli Syahputra², and Sri Fitria Retnawaty²

¹Department of Marine Sciences, Faculty of Fisheries Marine Sciences, Universitas Riau-Indonesia

²Department of Physics, Faculty of Mathematics, Natural Sciences and Health Sciences, Universitas Muhammadiyah Riau-Indonesia

Received: 2021-10-03

Accepted: 2022-04-27

Keywords:

Singapore Strait;
Sea surface temperature;
Rainfall

Correspondent email:

mubarak@lecturer.unri.ac.id

Abstract. Studying Singapore Strait waters condition as a form of maritime mitigation is necessary because it is an international shipping lane. The dominant weather changes include rainfall, wind flows, and sea surface temperature (SST). This study aims to reveal the relationship between rainfall and SST activity in the Singapore Strait for over 18 years, from 2002 to 2019. The results showed a negative correlation, where the SST decreases as rainfall increases and vice versa. In addition, the high rainfall and low SST distribution occur in the Western season (December–February). The low rainfall intensity and high (warm) SST distribution occur yearly in the transition from West to East (March–August). Also, the distribution pattern is influenced by rainfall intensity and the water mass from the South China Sea and the Malacca Strait, where the strait is a mixture of these masses. The neural network model confirmed the negative correlation. Hence a small change in SST causes rainfall if it is cooler, and less precipitation if warmer.

©2022 by the authors. Licensee Indonesian Journal of Geography, Indonesia.
This article is an open access article distributed under the terms and conditions of the Creative Commons Attribution (CC BY NC) license <https://creativecommons.org/licenses/by-nc/4.0/>.

1. Introduction

The Singapore Strait waters are between the Malacca Strait's water masses and the South China Sea. Furthermore, the rainy and dry seasons are experienced yearly, with maximum and minimum rain occurring in December–January and June–August, respectively (Sun et al., 2017; Sundarambal et al., 2009). The changes in rainfall intensity globally are due to El Nino (Isa et al., 2020), which causes variation in seawater temperature depending on the natural conditions affecting these waters. These changes occur daily, seasonal, annual, and long-term, especially in the surface layer (Thirumalai et al., 2017).

Despite being a sea transportation route, the Singapore Strait waters are used by traditional fishermen as a fishing area (Corpus, 2014). Meanwhile, knowledge about sea surface temperature (SST) distribution in waters is vital, including in fisheries and environmental management (Fu et al., 2020; Sukresno et al., 2021; Ciani et al., 2020). SST was a significant factor for fish migration in the fisheries industries, where fish colonies migrate from cold to warmer seas (Kiyofuji et al., 2019; Kristensen et al., 2020). It plays a role in precipitation intensity through global teleconnection (Alhamsry et al., 2019).

SST is an important oceanographic factor that drives the seasonal cycle in tropical and subtropical areas (Evans et al., 2000; Song et al., 2009). In addition, several studies reported the relationship between SST and rainfall on a global scale, leading to less explanation in small regions, such as the strait zone. The Singapore Strait's SST is believed to correlate with the rainy seasons in the nearest regions, such as Singapore

and Indonesia, specifically Riau Archipelago and eastern Sumatra Island.

This study aims to investigate the trend and pattern of rainfall to SST. The prime data was obtained using satellite imagery of Aqua-MODIS. Also, a neural network (NN) analysis was used to investigate rainfall trends for cooler and warmer conditions. Data and information were provided on the trend and pattern of SST for each season.

2. Methods

Study Area

Figure 1 shows that the Singapore Strait is located at 103° 18'57.24" to 104° 33'26.64" east longitude and 0° 54'16.42" to 1° 32'59.28" north latitude. The strait covers about 10,041.25 km² (Sundarambal et al., 2009). Furthermore, a detailed analysis focused on the waters of the Singapore Strait, where the changes in SST are influenced by the confluence between the water mass of the South China Sea and the Malacca Strait.

General Condition of Singapore Strait Waters

The Singapore Strait waters are semi-closed and connect the western South China Sea with the East Malacca Strait (Sun et al., 2017). In addition, these waters are a link between Indonesia, Singapore, and Malaysia. The climate phenomena that impact Indonesia and the waters of the Singapore Strait include El Nino Southern Oscillation and Indian Ocean Dipole (Maruyama et al., 2011; Gnanaseelan et

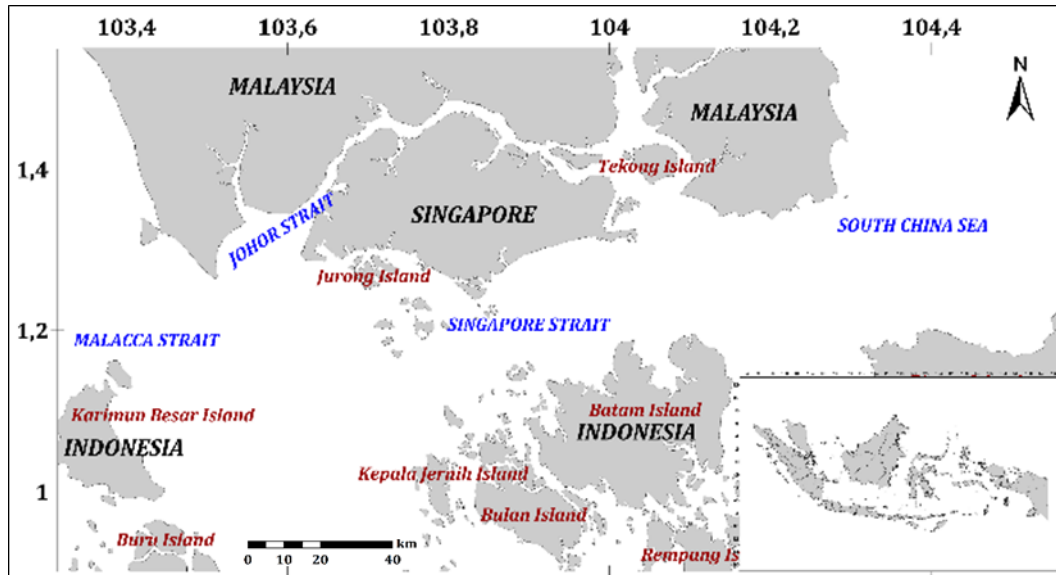


Figure 1. Maps of the study site

al., 2012; Hendrawan et al., 2019; Mubarak and Nurhuda, 2021). Geographically, the waters of the strait are between the Pacific and the Indian Ocean, which can affect the SST value phenomenon (Terray and Dominiak, 2005).

The SST characteristics of the Singapore Strait waters are similar to other waters in Indonesia, where the monthly SST values for the last three years ranged from 28.2°C to 32.2°C. As a tropical region, the strait water is covered by sunlight the whole year; hence, the fluctuation of SST is distinguishable as reported in Indonesia waters, ranging from 26°C to 31°C (Ray and Susanto, 2016).

Data Retrievals

Raw data of SST were retrieved from the satellite Aqua-MODIS Level 3 SST Imagery from 2002 to 2019 with a spatial resolution of 4 × 4 km. The data were downloaded from the NASA website (<http://oceancolor.gsfc.nasa.gov/>) as Hierarchical Data Format, while other rainfall data were collected from Batam Hang Nadim Airport during the period.

Image data processing interprets image or image data into the desired output. The SST value of the Aqua-MODIS image was based on the Miami Pathfinder Sea Surface Temperature algorithm (Luo et al., 2019; Currie et al., 2013). Furthermore, the SeaWiFS Data Analysis System (SeaDAS 7.2) software displayed the extracted SST image. Based on the study location, the image processing stage begins with cropping.

The Export Mask Pixels process runs the SST image cut to obtain the SST value. This value is obtained in the form of the American Standard Code for Information Interchange, based on the latitude and longitude position. The spreadsheet program was used to calculate the average monthly values, which was displayed as a time-series graph. Furthermore, the values were grouped by month and processed using the Surfer 11 software to obtain a monthly average SST distribution map. The monthly average SST values based on latitude and longitude positions were stored as a '*.grd' file using Surfer 11 to obtain the distribution map. The map obtained was stored in JPEG format for easy visual observation.

NN Analysis

Several studies used the NN analysis to predict and forecast weather to stoke the market. Meanwhile, NN in 'nntool' of Matlab® was applied using open-accessed data from Climate Research Unit (CRU) database from 2002 to 2019. The network was trained under the Bayesian regulation function using the data as a baseline. In addition, the SST is treated under two schemes, i.e. warming (+0.5 and +1.0 °C) and cooling conditions (-0.5 and -1.0 °C).

3. Results and Discussion

Temporal Variability of SST

Figure 2 shows the SST's temporal variation over the last three years. The highest average was in May 2019, and the lowest was in February 2017 and December 2019, with an average temperature of 32.2°C and 28.2°C, respectively. Also, the average monthly value varied with a tendency to increase, where the SST was higher from April to June and lowered from December to March.

Figure 3 illustrates the increasing annual SST fluctuation in the West season (i.e. December). The tropical sea surface layer conditions are warm, with small annual temperature variations, and the daily temperature variations are lower than subtropics (Xu et al., 2021). Also, tropical waters' annual mean temperature variation is less than 2°C at the equator (Tuchen et al., 2020; Shaltout, 2019).

The increase in SST in Singapore Strait is about 0.0502 °C/year, as presented by the linear regression plot in Figure 3. Therefore, this is higher than the average warming trend in the Mediterranean sea of 0.036 °C/year (Pastor et al., 2017) and slightly lower than the SST trend in the Red Sea from 2005 to 2016 (Shaltout, 2019). This is because the strait lies in a tropical zone and directly connects with the Pacific and Indian oceans.

Spatial Distribution of SST

Figure 4 depicts the average monthly and seasonal spatial distribution profile of SST in the Singapore Strait waters. The distribution demonstrated that it varies based on the season, with the offshore waters being warmer than

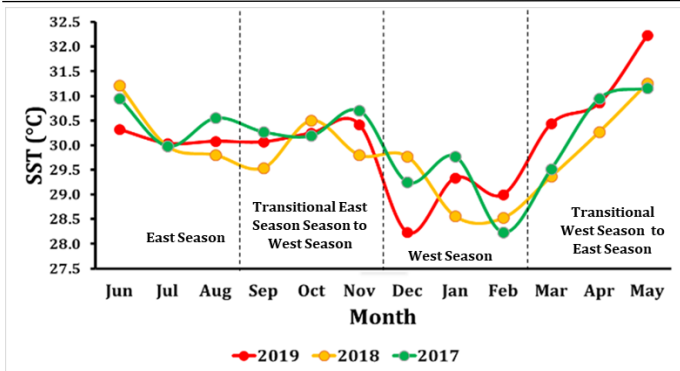


Figure 2. Graph of the mean monthly SST temporal variability for four seasons

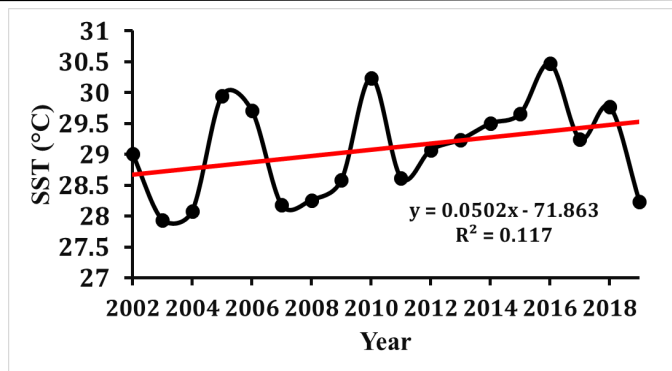


Figure 3. Graph of annual SST trends in the West season for 18 years

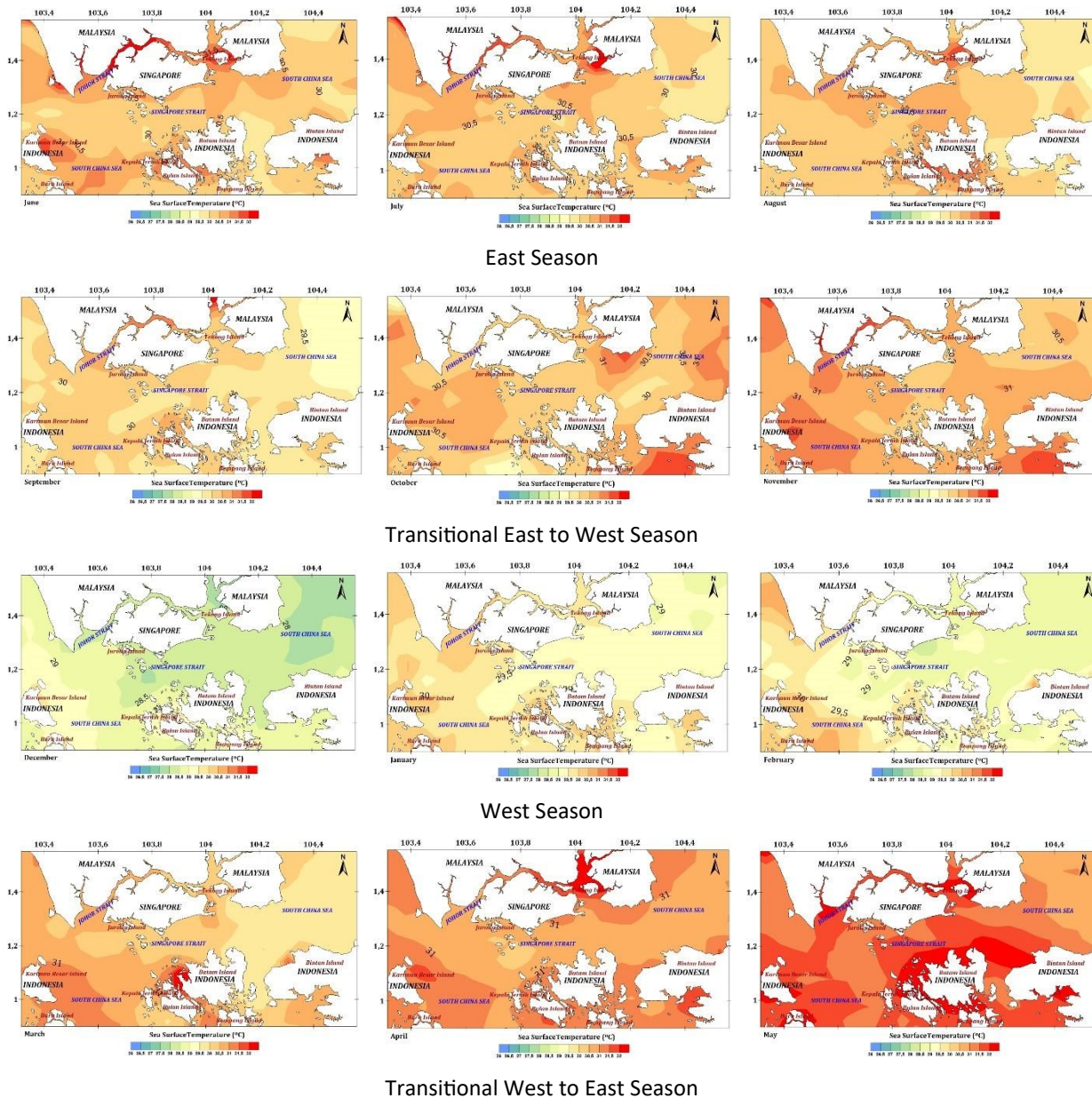


Figure 4. Spatial distribution of average monthly SST in the waters of the Singapore Strait

the near-shore. According to Li et al. (2019), land temperatures affect those around the coastline. The SST is evenly distributed or with relatively small variations in certain months.

The average monthly SST from the East monsoon to the East to West transitional season shows a stable spatial distribution, with a dominating temperature range of 30°C–

32°C. Furthermore, the strait is warmer in the Eastern season compared to other seasons, where the sun's radiation intensity ranges from moderate to high.

The SST in the West and West to East transitional seasons indicates that the spatial distribution varies from low to high temperatures, specifically in February and March. This occurs in the temperature range of 28°C–30.5°

C. In February, a small region of offshore waters (far from the coast) had temperatures above 28.5°C in February, which is the end of the Western season (Fig. 5). However, it is warm in March, the beginning of the West to East transition season. The average SST ranges from 30°C–32°C and 29°C–30°C in areas closer to the coast and offshore waters, respectively. In addition, the SST conditions are warm during the year because the waters are in the tropics, close to the equator. The seasonal changes have impacted the SST values, though with a small level of fluctuation.

The East monsoon has a higher SST fluctuation pattern than the West, with fluctuating patterns which last for three months seasonally (Antoni et al., 2019; Soeriaatmadja, 2008). This monthly variation resembles that of the South China Sea.

According to Thiébaux et al. (2003), the high SST in the East monsoon and part of the East to West transitional season is due to the sun’s position, which has adjusted to the Northern Hemisphere. Therefore, the Northern Hemisphere has high temperatures with low air pressure, specifically the Asian continent.

Correlation of Rainfall and SST

The monthly correlation of rainfall and SST in the Singapore Strait region shows various correlation coefficient values. Figure 6 illustrates that the SST zone with the highest correlation coefficient value is diverse distribution. There is a relationship between rainfall and SST based on the distribution of the values.

The conducted analysis showed a negative correlation response, indicating a high increase in rainfall in areas with a decrease in SST. Hence, the rainfall intensity is related to anomalous changes in SST (Dewi et al., 2020; Nababan et al.,

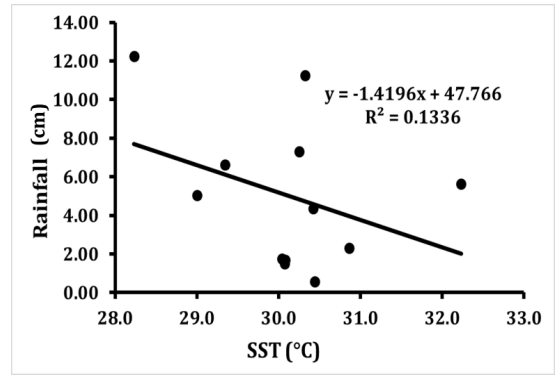


Figure 5. Average annual rainfall and SST for the period 2002–2019

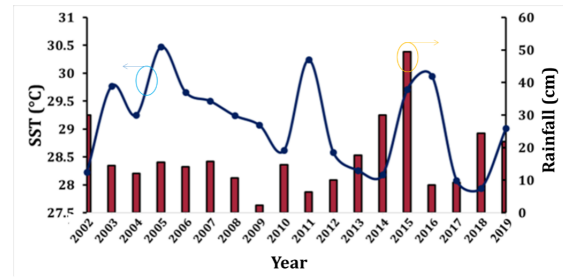


Figure 6. Correlation between rainfall and annual SST for the period 2002–2019

2016). According to Nababan et al. (2016), the negative anomaly of the average monthly SST value during the transition season of the West to East monsoons and the East monsoon begins in May, obtains a minimum level in August, and ends in October.

The SST level occurring in the waters of the Singapore Strait is influenced by rainfall and the conditions of the circulation patterns of seasonal winds and currents.

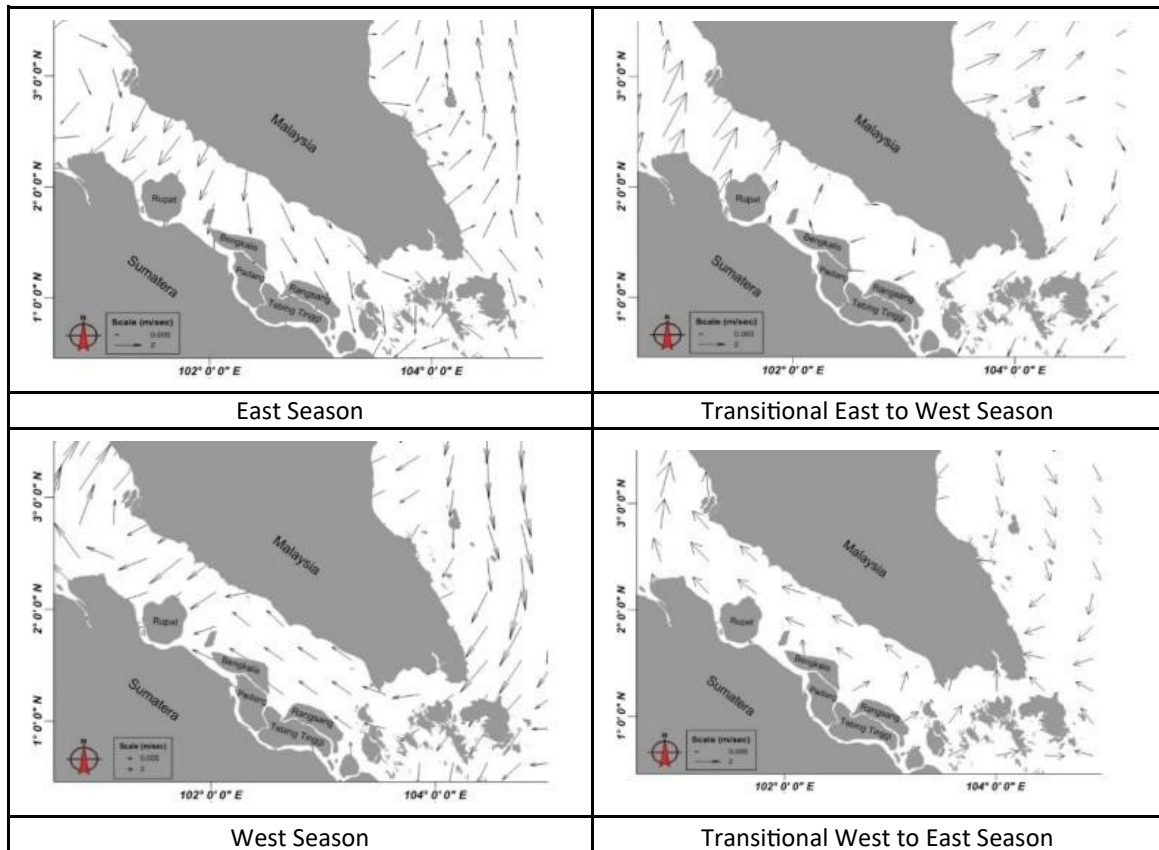


Figure 7. Seasonal current circulation pattern in the Singapore Strait waters

According to Nababan et al. (2016), SST variability is affected by meteorological conditions (precipitation, evaporation, humidity, air temperature, wind speed, and solar radiation intensity) and oceanographic processes (Sherwen et al., 2019; Jena et al., 2020; Merchant et al., 2019; Chaidez et al., 2017).

The winds and ocean currents occurring in the Singapore Strait in the West monsoon period originate from the South China Sea (Mubarak et al., 2017; Nurhuda et al., 2019). In addition, the winds and currents moving from the North and South China Sea generate water vapour that is cool enough to allow the Singapore Strait to experience the rainy season, or SST will be low than other seasons (Fig. 7).

Pramuwardani et al. (2018) reported that the surface wind circulation pattern in the Northern Hemisphere moves to the Southern region. The current movement pattern from the South China Sea to the Malacca Strait is through the Singapore Strait (Endo and Kitoh, 2014). This pattern supports the phenomenon of SST distribution in the Malacca Strait and its surroundings, including the Singapore Strait, which is cooler. In the East monsoon, the current circulation pattern moves from the Malacca Strait through the Singapore Strait to the South China Sea (Antoni et al., 2019). Consequently, the SST distribution in the waters of the Singapore Strait is warm during this period.

Rainfall Pattern to Variable SST

Figure 8 shows the trained model of NN for the dataset. The model is fitted to baseline data with a precision coefficient of $R=92.16\%$. Therefore, there are indications

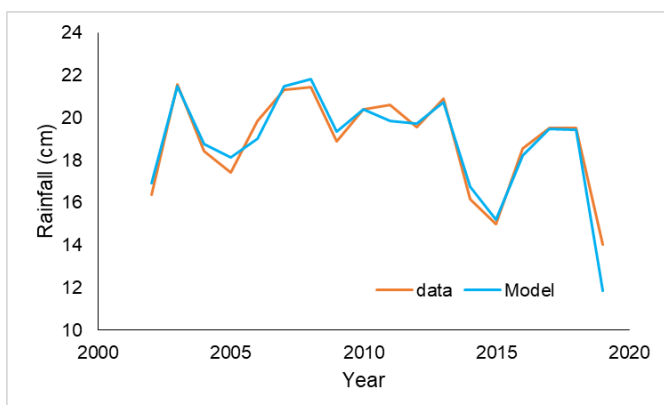


Figure 8. Comparison of rainfall dataset dan NN model

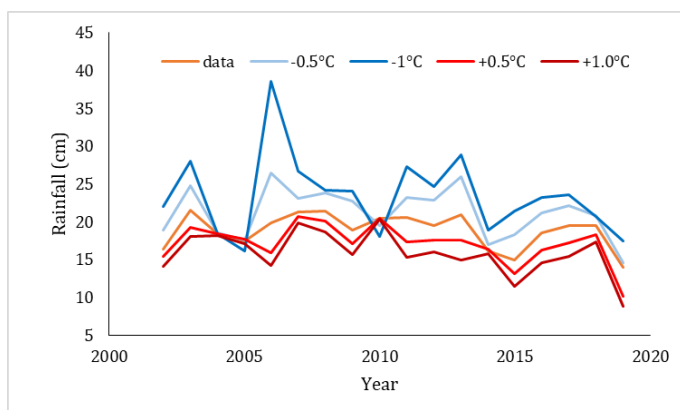


Figure 9. Precipitation sensitivity under cooler and warmer SST of Singapore Strait

that cooler SST in Singapore Strait influences higher rainfall intensity and vice versa.

The simulation data confirmed inverse correlation, as suggested in Figure 4. Furthermore, the coefficient correlation was 0.1336, indicating that the primary precipitation source is not from the Strait water and is unrelated to the SST. Alhamsry et al. (2019) stated that SST changes in the southern Pacific and northern Atlantic caused precipitation activity in Ethiopia. Figure 9 showed that precipitation in the strait is triggered by a low correlation between SST and rainfall. Consequently, a longer drought season in the Singapore Strait region and Southeast Asia is triggered by global warming.

4. Conclusion

The global SST tends to rise in narrow waters such as Singapore Strait. Also, the distribution pattern had a negative correlation with rainfall in the monthly, seasonal, and annual series. The SST is influenced by rainfall intensity and water masses originating from the South China Sea and the Malacca Strait. In addition, the monthly and annual distribution patterns indicated that the water mass is a mixture of the South China Sea and Malacca Strait. The NN model showed that SST influences the rainfall trend.

Acknowledgement

The author is grateful to the Institute for Research and Community Service (LPPM) of Universitas Riau for the generous financial support. Also, the comparison data presented were sourced from the CRU database (<https://www.cru.uea.ac.uk/data>).

References

- Alhamsry, A., Fenta, A. A., Yasuda, H., Kimura, R., & Shimizu, K. (2019). Seasonal Rainfall Variability in Ethiopia and Its Long-Term Link to Global Sea Surface Temperatures. *Water*, 12(1), 55. <https://doi.org/10.3390/w12010055>
- Antoni, S., Bantan, R. A., Al-Dubai, T. A., Lubis, M. Z., Anurogo, W., & Silaban, R. D. (2019). Chlorophyll-a, and Sea Surface Temperature (SST) as proxies for Climate Changes: Case Study in Batu Ampar waters, Riau Islands. *IOP Conference Series: Earth and Environmental Science*, 273(1), 012012. <https://doi.org/10.1088/1755-1315/273/1/012012>
- Chaidez, V., Dreano, D., Agusti, S., Duarte, C. M., & Hoteit, I. (2017). Decadal trends in Red Sea maximum surface temperature. *Scientific Reports*, 7(1). <https://doi.org/10.1038/s41598-017-08146-z>
- Ciani, D., Rio, M. H., Nardelli, B. B., Etienne, H., & Santoleri, R. (2020). Improving the Altimeter-Derived Surface Currents Using Sea Surface Temperature (SST) Data: A Sensitivity Study to SST Products. *Remote Sensing*, 12(10), 1601. <https://doi.org/10.3390/rs12101601>
- Corpus, L. (2014). Reconstructing Singapore's marine fisheries catch, 1950-2010. In K. Zylich, D. Zeller, M. Ang, & D. Pauly (Eds.), *Fisheries catch reconstructions: Islands, Part IV, Fisheries Centre Research Reports*, (22(2), pp. 137-146). Vancouver, Canada: University of British Columbia.
- Dewi, Y. W., Wirasatriya, A., Sugianto, D. N., Helmi, M., Marwoto, J., & Maslukah, L. (2020). Effect of ENSO and IOD on the Variability of Sea Surface Temperature (SST) in Java Sea. *IOP Conference Series: Earth and Environmental Science*, 530(1), 012007. <https://doi.org/10.1088/1755-1315/530/1/012007>
- Endo, H., & Kitoh, A. (2014). Thermodynamic and dynamic effects on regional monsoon rainfall changes in a warmer climate. *Geophysical Research Letters*, 41(5), 1704–1711. <https://doi.org/10.1002/2013GL058111>

- doi.org/10.1002/2013gl059158
- Evans, M. N., Kaplan, A., & Cane, M. A. (2000). Intercomparison of coral oxygen isotope data and historical sea surface temperature (SST): Potential for coral-based SST field reconstructions. *Paleoceanography*, *15*(5), 551–563. <https://doi.org/10.1029/2000pa000498>
- Fu, A., Patil, K. R., & Iiyama, M. (2020). Region Proposal and Regression Network for Fishing Spots Detection from Sea Temperature. *Global Oceans 2020: Singapore – U.S. Gulf Coast*. <https://doi.org/10.1109/ieeeconf38699.2020.9389050>
- Gnanaseelan, C., Deshpande, A., & McPhaden, M. J. (2012). Impact of Indian Ocean Dipole and El Niño/Southern Oscillation wind-forcing on the Wyrkti jets. *Journal of Geophysical Research: Oceans*, *117*(C8), n/a. <https://doi.org/10.1029/2012jc007918>
- Hendrawan, I. G., Asai, K., Triwahyuni, A., & Lestari, D. V. (2019). The interannual rainfall variability in Indonesia corresponding to El Niño Southern Oscillation and Indian Ocean Dipole. *Acta Oceanologica Sinica*, *38*(7), 57–66. <https://doi.org/10.1007/s13131-019-1457-1>
- Isa, N. S., Akhir, M. F., Kok, P. H., Daud, N. R., Khalil, I., & Roseli, N. H. (2020). Spatial and temporal variability of sea surface temperature during El-Niño Southern Oscillation and Indian Ocean Dipole in the Strait of Malacca and Andaman Sea. *Regional Studies in Marine Science*, *39*, 101402. <https://doi.org/10.1016/j.rsma.2020.101402>
- Jena, P., Kasiviswanathan, K. S., & Azad, S. (2020). Spatiotemporal characteristics of extreme droughts and their association with sea surface temperature over the Cauvery River basin, India. *Natural Hazards*, *104*(3), 2239–2259. <https://doi.org/10.1007/s11069-020-04270-8>
- Kiyofuji, H., Aoki, Y., Kinoshita, J., Okamoto, S., Masujima, M., Matsumoto, T., Fujioka, K., Ogata, R., Nakao, T., Sugimoto, N., & Kitagawa, T. (2019). Northward migration dynamics of skipjack tuna (*Katsuwonus pelamis*) associated with the lower thermal limit in the western Pacific Ocean. *Progress in Oceanography*, *175*, 55–67. <https://doi.org/10.1016/j.pocean.2019.03.006>
- Kristensen, M., Righton, D., del Villar-Guerra, D., Baktoft, H., & Aarestrup, K. (2018). Temperature and depth preferences of adult sea trout *Salmo trutta* during the marine migration phase. *Marine Ecology Progress Series*, *599*, 209–224. <https://doi.org/10.3354/meps12618>
- Li, J., Li, X., Li, X., Chen, L., & Jin, L. (2019). Observed Multi-Timescale Differences between Summertime Near-Surface Equivalent Temperature and Temperature for China and Their Linkage with Global Sea Surface Temperatures. *Atmosphere*, *10*(8), 447. <https://doi.org/10.3390/atmos10080447>
- Luo, B., Minnett, P. J., Gentemann, C., & Szczodrak, G. (2019). Improving satellite retrieved night-time infrared sea surface temperatures in aerosol contaminated regions. *Remote Sensing of Environment*, *223*, 8–20. <https://doi.org/10.1016/j.rse.2019.01.009>
- Maruyama, F., Kai, K., & Morimoto, H. (2011). Wavelet-Based Multifractional Analysis of the El Niño/Southern Oscillation, the Indian Ocean Dipole and the North Atlantic Oscillation. *SOLA*, *7*, 65–68. <https://doi.org/10.2151/sola.2011-017>
- Merchant, C. J., Embury, O., Bulgin, C. E., Block, T., Corlett, G. K., Fiedler, E., Good, S. A., Mittaz, J., Rayner, N. A., Berry, D., Eastwood, S., Taylor, M., Tsushima, Y., Waterfall, A., Wilson, R., & Donlon, C. (2019). Satellite-based time-series of sea-surface temperature since 1981 for climate applications. *Scientific Data*, *6*(1). <https://doi.org/10.1038/s41597-019-0236-x>
- Mubarak, M., & Nurhuda, A. (2021). Sediment Movements in Estuary of Siak River, Riau Basin, Indonesia. *Indonesian Journal of Geography*, *53*(1). <https://doi.org/10.22146/ijg.57100>
- Mubarak, Sulaiman, A., & Efriyeldi. (2017). Environmental Effect of Tidal Bore Propagation in Kampar River. *MATEC Web of Conferences*, *103*, 04015. <https://doi.org/10.1051/mateconf/201710304015>
- Nababan, B., Rosyadi, N., Manurung, D., Natih, N. M., & Hakim, R. (2016). The Seasonal Variability of Sea Surface Temperature and Chlorophyll-a Concentration in the South of Makassar Strait. *Procedia Environmental Sciences*, *33*, 583–599. <https://doi.org/10.1016/j.proenv.2016.03.112>
- Nurhuda, A., Mubarak, M., & Sutikno, S. (2019). Analysis of coastal vulnerability of Rangsang Island due to climate changes. *Journal of Degraded and Mining Lands Management*, *6*(4), 1907–1914. <https://doi.org/10.15243/jdmlm.2019.064.1907>
- Pastor, F., Valiente, J. A., & Palau, J. L. (2017). Sea Surface Temperature in the Mediterranean: Trends and Spatial Patterns (1982–2016). *Pure and Applied Geophysics*, *175*(11), 4017–4029. <https://doi.org/10.1007/s00024-017-1739-z>
- Pramuwardani, I., Hartono, Sunarto, & Sopaheluwakan, A. (2018). Indonesian rainfall variability during Western North Pacific and Australian monsoon phase related to convectively coupled equatorial waves. *Arabian Journal of Geosciences*, *11*(21). <https://doi.org/10.1007/s12517-018-4003-7>
- Ray, R. D., & Susanto, R. D. (2016). Tidal mixing signatures in the Indonesian seas from high-resolution sea surface temperature data. *Geophysical Research Letters*, *43*(15), 8115–8123. <https://doi.org/10.1002/2016gl069485>
- Shaltout, M. (2019). Recent sea surface temperature trends and future scenarios for the Red Sea. *Oceanologia*, *61*(4), 484–504. <https://doi.org/10.1016/j.oceano.2019.05.002>
- Sherwen, T., Chance, R. J., Tinel, L., Ellis, D., Evans, M. J., & Carpenter, L. J. (2019). A machine-learning-based global sea-surface iodide distribution. *Earth System Science Data*, *11*(3), 1239–1262. <https://doi.org/10.5194/essd-11-1239-2019>
- Soeriaatmadja, R. E. (2008). Surface Salinities in the Strait of Malacca. *Marine Research in Indonesia*, *2*, 27–55. <https://doi.org/10.14203/mri.v2i0.326>
- Song, D., Bao, X., Wang, X. H., & Wu, W. (2009). The optimization algorithm for the pathfinder sea surface temperature in the East China Seas. *Ocean Science Journal*, *44*(1), 11–19. <https://doi.org/10.1007/s12601-009-0002-7>
- Sukresno, B., Jatisworo, D., & Hanintyo, R. (2021). Validation of Sea Surface Temperature from GCOM-C Satellite Using iQuam Datasets and MUR-SST in Indonesian Waters. *Indonesian Journal of Geography*, *53*(1). <https://doi.org/10.22146/ijg.53790>
- Sun, Y., Eltahir, E., & Malanotte-Rizzoli, P. (2017). The bottom water exchange between the Singapore Strait and the West Johor Strait. *Continental Shelf Research*, *145*, 32–42. <https://doi.org/10.1016/j.csr.2017.07.004>
- Sundarambal, P., Balasubramanian, R., & Tklich, P. (2009). Atmospheric fluxes of nutrients onto Singapore Strait. *Water Science and Technology*, *59*(11), 2287–2295. <https://doi.org/10.2166/wst.2009.262>
- Terray, P., & Dominiak, S. (2005). Indian Ocean Sea Surface Temperature and El Niño–Southern Oscillation: A New Perspective. *Journal of Climate*, *18*(9), 1351–1368. <https://doi.org/10.1175/jcli3338.1>
- Thiébaux, J., Rogers, E., Wang, W., & Katz, B. (2003). A New High-Resolution Blended Real-Time Global Sea Surface Temperature Analysis. *Bulletin of the American Meteorological Society*, *84*(5), 645–656. <https://doi.org/10.1175/bams-84-5-645>
- Thirumalai, K., DiNezio, P. N., Okumura, Y., & Deser, C. (2017). Extreme temperatures in Southeast Asia caused by El Niño and worsened by global warming. *Nature Communications*, *8*(1). <https://doi.org/10.1038/ncomms15531>
- Tuchen, F. P., Lübbecke, J. F., Brandt, P., & Fu, Y. (2020). Observed Transport Variability of the Atlantic Subtropical Cells and Their Connection to Tropical Sea Surface Temperature Variability. *Journal of Geophysical Research: Oceans*, *125*(12). <https://doi.org/10.1029/2020jc016592>
- Wisetya Dewi, Y., Wirasatriya, A., Nugroho Sugianto, D., Helmi, M., Marwoto, J., & Maslukah, L. (2020). Effect of ENSO and IOD on the Variability of Sea Surface Temperature (SST) in Java Sea.

IOP Conference Series: Earth and Environmental Science, 530
(1), 012007. <https://doi.org/10.1088/1755-1315/530/1/012007>

Xu, F., Du, Y. A., Chen, H., & Zhu, J. M. (2021). Prediction of Fish Migration Caused by Ocean Warming Based on SARIMA Model. *Complexity*, 2021, 1–9. <https://doi.org/10.1155/2021/5553935>